Complete momentum balance for single ionization of helium by fast ion impact: Experiment

R. Moshammer,[1] J. Ullrich,[2] H. Kollmus,[1] W. Schmitt,[2] M. Unverzagt,[1] H. Schmidt-Böcking,[1] C. J. Wood,[3] and R. E. Olson[3]
[1]*Institut für Kernphysik, August-Euler-Strasse 6, D-60486 Frankfurt, Germany*
[2]*Gesellschaft für Schwerionenforschung, m.b.H., Planckstrasse 1, D-64291 Darmstadt, Germany*
[3]*Department of Physics, University of Missouri-Rolla, Rolla, Missouri 65401*
(Received 11 February 1997)

The collision dynamics of He single ionization by 3.6 MeV/u Se^{28+} impact was explored using the reaction microscope of the Gesellschaft für Schwerionenforschung, a high-resolution integrated multielectron recoil-ion momentum spectrometer. The complete three-particle final-state momentum distribution (nine Cartesian components p_i) was imaged with a resolution of $\Delta p_i \approx \pm 0.1$ a.u. by measuring the three momentum components of the emitted electron and the recoiling target ion in coincidence. The projectile energy loss has been determined on a level of $\Delta E_p/E_p \approx 10^{-7}$ and projectile scattering angles as small as $\Delta\vartheta \approx 10^{-7}$ rad became accessible. The experimental data which are compared with results of classical trajectory Monte Carlo calculations reveal an unprecedented insight into the details of the electron emission and the collision dynamics for ionization of helium by fast heavy-ion impact. [S1050-2947(97)01908-2]

PACS number(s): 34.10+x, 34.50.Fa

I. INTRODUCTION

When energetic charged projectiles interact with neutral atoms, the ejection of a target electron is the dominant reaction channel occurring with cross sections on the order of 10^{-15} cm^2. The detailed understanding of the facets of target ionization, therefore, has a strong impact on any application which is based on energy deposition in matter by fast ions. Among them are the radiation damage of biological and other materials, track formation and bulk modifications, the development of radiation detection devices, and the investigation of plasmas. One important source of systematic data contributing to our understanding of the collision dynamics are measurements of ionization cross sections doubly differential in ejected electron energy and angle (for a review see, e.g., [1]). As stated in [1], however, there are only a few sets of reliable data for the emission of low-energy electrons (see, e.g., [2,3]) with energies below 20 eV which contribute about 50% to the total single-ionization cross section. In addition, most of these investigations were performed using low-charged projectiles such as electrons [4] and protons [5]. Recently, highly charged heavy ions (for an upcoming review on existing data see [6]) gained increasing interest concerning applicational aspects in connection with the cancer therapy project at the Gesellschaft für Schwerionenforschung (GSI) [7].

Despite its outstanding importance, no kinematically complete experimental investigation has been published that provides information on the electron emission, the recoil-ion scattering, and the energy loss, as well as the angular straggling of the projectile for single ionization by ion impact. Only one study has been presented recently where the longitudinal momentum balance was completely determined [8]. In contrast, single ionization by electron impact has been extensively investigated in kinematically complete so-called $(e,2e)$ experiments (for a review see [4]). Even for double photoionization a considerable amount of kinematically complete $(\gamma,2e)$ studies have been performed since the pioneering experiment [9] in 1993.

The complete lack of such data for ion impact is due to two reasons: First, for most collision systems the change in projectile energy and transverse momentum (scattering angle) in a typical ionization encounter is by far smaller than the momentum spread of ion beams from modern accelerators or even storage rings where the ions are cooled by the interaction with electrons or lasers. Thus, the momentum change of the projectile has only been accessible experimentally with sufficient resolution for light (hydrogen, helium) and slow ($E_p < 500$ keV) ions (see, e.g., [10]). One study has been performed for 2.1 MeV/u C^{6+} on Ne where the relative energy loss as well as the projectile scattering has been measured for neon multiple ionization [11,12]. In a few other experiments projectile scattering angles have been detected in coincidence only with the emitted electron (see, e.g., [13]), the recoil-ion charge state [13,14], and its transverse momentum [15–18]. All these studies severely suffered from limited resolution.

Second, conventional electron spectroscopy, where the energy distribution of secondary electrons is scanned step by step in energy and angle, faces tremendous difficulties in the detection of slow electrons [1] and, more importantly, suffers from small solid angles on the order of 10^{-3} of 4π. Both are severe restrictions, because most of the emitted electrons are soft electrons which contribute significantly to the total cross section, and measurements coincident with the projectile or the recoil ion are extremely difficult [13]. Usually, neither the charge state of the recoil ion nor that of the outgoing projectile is determined.

Due to these reasons the only possible strategy leading to kinematically complete experiments is the coincident, charge state selective detection of the recoiling target ion and the emitted electron where the final momenta of both are determined with sufficient resolution. Experimentally this is a challenging task since, as mentioned before, nearly 50% of the electrons are emitted with energies below 20 eV and the recoiling target ions of interest have energies in the sub-meV regime. Only during the last few years efficient recoil-ion detection techniques have been developed, based on ultracold supersonic jet targets, which are sensitive to such small

energy transfers to the target nucleus (see, e.g., [19–22] and for an upcoming review see [23]). Moreover, efficient methods for the detection of low-energy electrons have been developed recently at GSI [8,24]. By using a superposition of electric and solenoidal magnetic fields all electrons with energies below 50 eV including for the first time those with $E_e = 0$ eV were projected on large area position sensitive detectors. From their position and time of flight (TOF), measured in an electron recoil-ion projectile coincidence, their trajectory has been calculated and, thus, their initial momentum vector (all three spatial dimensions) was obtained. (Similar projection techniques have been applied more recently providing either only the total energy of the electrons [25] or two out of three momentum components [26,27].) Up to now only longitudinal momentum balances have been published since the transverse recoil-ion momentum resolution was limited to 0.5 a.u. in these first experiments. In this paper we report on the kinematically complete experimental study of target single ionization by ion impact with a resolution of $\Delta p_i \approx \pm 0.1$ a.u. for all nine final momentum components p_i. Single differential cross sections, as well as the complete momentum balance for the longitudinal and the transverse direction, are presented.

From the theoretical point of view considerable progress has been achieved within the last decade in the description of ionization collision dynamics on a quantum-mechanical basis (for a review see [28]) as well as with semiclassical treatments [29,30]. In the perturbative regime where the Born approximation is applicable, methods have been developed to calculate three-body kinematics [31–33]. In the nonperturbative regime the ''hidden crossing'' method [34] has been developed for slow, adiabatic collisions ($v_p < v_e$, v_p: projectile velocity, v_e: velocity of the active electron). More recently the time dependent Schrödinger equation of the electron in the field of the two nuclei moving on classical trajectories has been solved numerically by discretization using a Cartesian mesh [35,36]. In both methods, however, the projectile motion is separated and approximated by a straight line.

At higher projectile velocities ($v_p > v_e$) for nonperturbative collisions ($q/v_p > 1$, q: projectile charge) three-body interactions also termed ''two-center effects'' strongly influence the electron emission characteristics [6,37]. Very low-energy electrons were found to be emitted into the forward direction due to the ''postcollision interaction'' with the emerging projectile [8,38,39]. In addition, as will be demonstrated in this paper, the projectile scattering can no longer be treated assuming a central interaction potential, but the complete three-particle problem has to be solved. Two-center effects on the electron emission have been included recently (for an overview see [28] and references therein) and total ionization cross sections as well as the details of the electron emission were successfully calculated (see also [40,41]). In the longitudinal direction even recoil-ion momenta as well as the momentum change of the projectile have been deduced from calculated electron momenta applying momentum conservation laws [42]. Since, however, the complete three-particle problem is not solved, the transverse scattering of the recoil ion and of the projectile is not accessible within this approach. Thus, the very fundamental three-particle problem, single ionization of a target atom by an ion in the nonperturbative regime (which is the most important one if slowing down of ions in matter is considered and which, in essence, leads to the Bragg maximum in the energy loss) is still out of the capabilities of most calculational techniques.

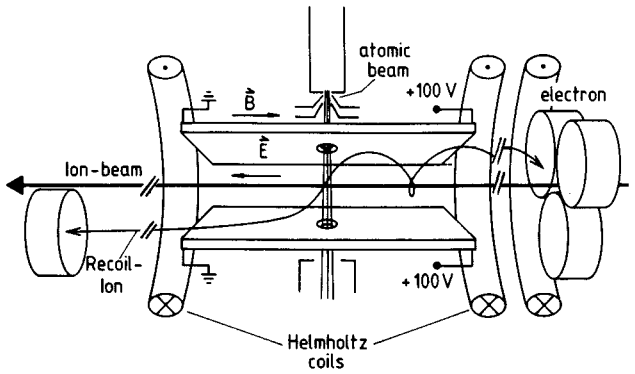

FIG. 1. Schematic drawing of the combined recoil-ion many-electron momentum spectrometer.

On the other hand tremendous progress has been achieved using semiclassical methods. Classical trajectory Monte Carlo (CTMC) calculations are the only method in the nonperturbative regime that treats the full three-particle problem without any approximation beyond classical scattering for the interaction of the charged particles. Quantum behavior is included statistically by using a momentum distribution of the electron in the bound state of the target atom determined by potentials based on Hartree-Fock calculations. Methods have been developed for treating many electron transitions (n-body CTMC) accounting for the electron-electron interaction in the ground state. More sophisticated techniques were reported to treat the (e-e) interaction during the collision accounting for the monopole part of the interaction (dynamical screening: dCTMC [43]) as well as on its direct implementation in the postcollision dynamics for transfer ionization and double ionization collisions [44].

II. EXPERIMENTAL METHOD

The recently developed combined multielectron recoil-ion momentum spectroscopy [24] was used to control and analyze with high resolution the reaction products after target ionization. One substantial part guaranteeing an internally cold and well defined He target is a two stage supersonic jet. The He gas expands through a 30 μm diameter nozzle forming a supersonic atomic beam. With two skimmers of 0.3 mm and 0.4 mm diameter, respectively, the innermost part of this beam is cut out providing a localized ($\Delta x \approx 2$ mm) and dense (10^{12} cm^{-2}) He target. The atomic beam is crossed with a well collimated beam (1 mm $\times$ 1 mm) of 3.6 MeV/u Se^{28+} ions delivered from the universal linear accelerator (UNILAC) at GSI. The projectiles were charge state analyzed after the collision and Se^{28+} ions (no charge exchange) were recorded by a fast scintillation counter with a rate up to 1 MHz. Recoiling target ions and electrons produced in the reaction zone are extracted along the ion beam into opposite directions by a weak uniform electric field of 1–5 V/cm applied over a length of 22 cm (Fig. 1). An additional homogenous magnetic field of typical 10–20 Gauss,

generated by two Helmholtz coils (1.5 m diameter), is applied almost parallel to the electric field which forces the electrons on cyclotron trajectories. In this way the electrons are efficiently guided onto the detector and a high detection solid angle is guaranteed. After acceleration in the electric-field recoil ions and electrons both drift over 22 cm before they are postaccelerated (2000 V for recoil ions and 200 V for electrons) and detected by two-dimensional position sensitive (2D PS) channel-plate detectors. With this focusing geometry the time of flight becomes independent in first order on the extension of the reaction zone considerably increasing the resolution in the longitudinal direction. From the position of detection and the TOF, measured in an electron recoil-ion projectile coincidence, the recoil-ion charge state and the three momentum components of both, the recoil ion and the emitted electron, can be deduced. All recoil ions of interest and all electrons ($\Delta\Omega=4\pi$ for energies up to 50 eV) are projected onto the detectors. Due to detector efficiencies and grid transmissions a total triple coincidence efficiency of about 20% was achieved. Details about the spectrometer, its advantages and limits, and how to extract unambiguously the trajectories and the initial momenta of the reaction products can be found in [24].

If a double-ionization event occurs one is faced with the problem that the position and the TOF of both electrons has to be recorded. This is not a simple task since both electrons hit the detector within a time gap of less than 200 ns. With our new three-fold electron detector device, which consists of three independent (2D PS) detectors [45], we can easily fulfill this requirement under the specific condition that each electron hits a different detector. If both electrons arrive at the same detector we lose the position information but we can still determine their time of arrival if their spacing in time is more than 8 ns. This allows us to extract the longitudinal momenta of both electrons in coincidence with the complete momentum vector of the He^{2+} recoil ion. Recent improvements of the electron spectrometer, time focusing, as well as the threefold detector, are described in more detail in [45]. Results of double ionization have partly been published [44] and will be discussed in a forthcoming publication.

Besides the unique advantage of a 4π solid angle and large momentum acceptance, which is necessary for coincidence measurements, our technique for low-energy electron detection removes many of the tremendous experimental difficulties of conventional spectrometers. The target extension is well defined by the supersonic jet. Electrons from the residual gas are completely suppressed in the triple coincidence spectra. The influence of electric fringe fields and magnetic distortions is drastically reduced by extracting the electrons. The final charge state of the target and that of the projectile ion are well defined. Furthermore, since the Q value of the reaction is measured in addition, simultaneous electronic excitation of the heavy projectile is excluded.

We want to emphasize, that for the investigation of multiple ionization or collision induced reactions where more than one electron is emitted, like in target ionization accompanied by electron loss from or electron capture to the projectile, large active diameter 2D PS electron detectors with fast multihit capable delay-line readout [46] will be implemented in the near future. This then allows kinematically complete experiments for a large variety of collision induced multiple-ionization reactions.

III. THEORETICAL MODEL

The experimental data presented here will be compared with results obtained with the CTMC theory. As mentioned in the Introduction, this theory treats the nonperturbative three-particle problem completely concerning the interactions between all particles, yielding the complete nine-dimensional final momentum space for single ionization. In this section we give a brief description of the theoretical model and shortly discuss the implemented improvements and its natural limits. The semiclassical model has been demonstrated to be an adequate approach to describe ion induced target single and multiple ionization for a large range of impact velocities and projectile charge states. Moreover, single electron capture from laser aligned initial states with the complete determination of product n, l, and ml quantal levels has been successfully benchmarked against experimental line emission measurements which includes polarization and anisotropy [47]. Recent studies for target single ionization of helium [8] and multiple ionization of neon [39] using fast heavy ions as well as investigations for slow highly charged ion and proton impact ionization of helium [26,27] demonstrated the capabilities of the CTMC approach. From an experimentalists point of view the fact that experimentally accessible highly differential cross sections can be calculated easily and in a clear manner is a further advantage.

The theoretical method used here includes inherently the three-particle dynamics: the interaction between all participating particles during and after the collision is directly incorporated in the calculations. The bound-electron initial state of helium is taken to be in a model potential determined from Hartree-Fock calculations. This same model potential is incorporated in the interaction of the projectile and the target nucleus so that all charges are asymptotically correct at both the separated and united atom limits. Moreover, the electron's Compton profile is in reasonable agreement with experimental values.

IV. RESULTS AND DISCUSSION

The dynamics of single ionization of an atom by charged particle impact is completely determined by the measurement of six out of nine momentum components of the three particles in the final state. The three missing momentum components as well as the inelasticity (the Q value) of the reaction can be deduced from momentum and energy conservation. For the overwhelming part of ion-atom collisions leading to ionization of the target atom only little momentum and energy compared to the initial momentum (p_P) and energy (E_P) of the incoming heavy projectile is transferred during the encounter. Under these conditions the longitudinal (along the ion-beam direction) and transverse momenta are decoupled and can be calculated separately on the basis of nonrelativistic energy and momentum conservation. Therefore, the transverse momentum balance in the laboratory frame of reference has to fulfill

$$\mathbf{p}_{R\perp}+\mathbf{p}_{e\perp}+\Delta\mathbf{p}_{P\perp}=0, \tag{1}$$

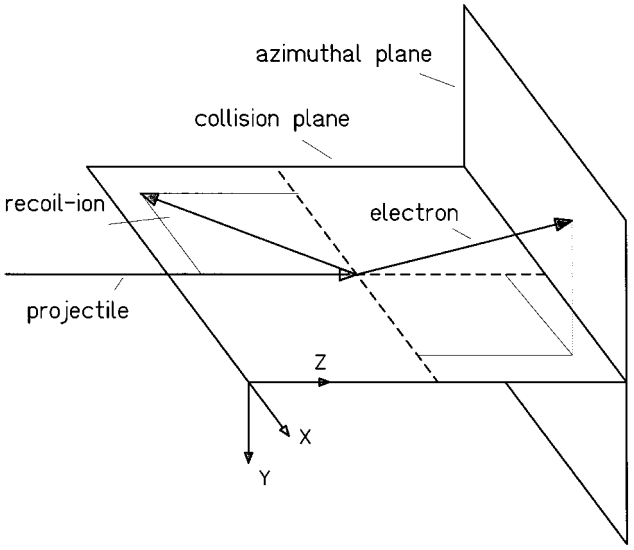

FIG. 2. Illustration of the collision geometry and declarations used throughout this paper.

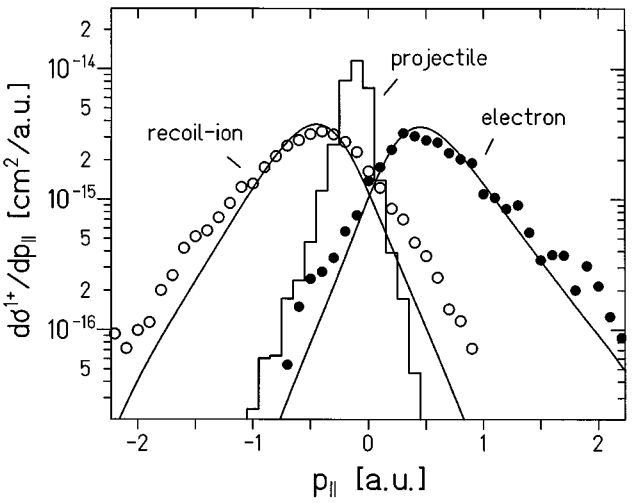

FIG. 3. Longitudinal momentum distributions of recoil ions and soft electrons together with the projectile's momentum loss (histogram). Smooth lines: CTMC calculation multiplied by a factor of 1.4.

with

$$|\Delta \mathbf{p}_{P\perp}| = \vartheta_P \sqrt{2 M_P E_P}. \tag{2}$$

(ϑ_P is the polar projectile scattering angle; M_P the projectile ion mass. $\mathbf{p}_{R\perp}$, $\mathbf{p}_{e\perp}$ are the final transverse recoil-ion and electron momentum vectors, respectively.) The longitudinal momentum balance is given by (in atomic units with $\hbar = e = m_e = 1$, m_e: electron mass, e: electron charge),

$$p_{R\parallel} + p_{e\parallel} - (Q + E_e)/v_P = 0 \tag{3}$$

and

$$\Delta p_{P\parallel} = -(Q + E_e)/v_P, \tag{4}$$

where v_P is the initial projectile velocity and $\Delta p_{P\parallel}$ the longitudinal momentum transfer. The inelasticity of the reaction $Q = (E_f^{bind} - E_i^{bind})$, the total difference in electronic energies between the initial and final atomic states, is directly connected to the longitudinal momentum transfer. Moreover, the longitudinal recoil-ion momentum is related to the continuum energy E_e of the ejected electron demonstrating the close linkage between recoil-ion momentum spectroscopy and electron spectroscopy [48].

Once the Q value is known, a quantity which is determined experimentally, then the process of single ionization is fully determined by the specification of a fivefold differential cross section. Several projections out of this many dimensional space onto specific physically relevant quantities will be discussed in order to elucidate the dynamics of collision induced ionization. Since all reaction products are detected simultaneously, the absolute cross section is easily obtained by normalizing the sum of all events to the measured total single-ionization cross section of $\sigma^{1+} = (3.3 \pm 0.5) \times 10^{-15}$ cm^2 [49]. This same value has been used to normalize the CTMC calculations which lie 27% below the accepted experimental value.

In this section experimental results for single ionization of helium due to the impact of 288 MeV (3.6 MeV/u) Se^{28+} will be discussed in detail and compared with results obtained by CTMC calculations. Since one cannot present all the possible projections and cuts out of the nine-dimensional momentum space (i.e., the square of the complete three-particle final-state wave function) a subjective selection of data is presented which in the authors opinion illuminates the main features of the underlying collision dynamics. Figure 2 illustrates the geometrical conventions used throughout this paper. The projectile moves along the z direction (this is the longitudinal direction). The transverse plane is the $(x$-$y)$ plane. The collision plane is defined by the incoming projectile vector and the recoil-ion transverse momentum going along the negative x direction (see Fig. 2).

A. Longitudinal momentum balance

The cross-section differential in longitudinal momenta of the recoil ion, the electron, and the projectile is shown in Fig. 3 together with predictions obtained from theory (lines). As in a previous measurement [8] with 3.6 MeV/u Ni^{24+} projectiles the electrons are found to be emitted dominantly into the forward direction with a most likely forward energy of only 2.5 eV. Their longitudinal momentum is almost completely balanced by the backscattered recoil ions. Thus, the projectile momentum change shows a narrow distribution whose width is mainly determined by our experimental resolution. Nevertheless, the tail on the left-hand side can be attributed to the electron energy distribution [the E_e/v_P term of Eq. (4)].

The target atom ''dissociates'' in the strong electric field of the passing projectile which delivers energy but only very little momentum. Therefore, the action of the fast heavy projectile reveals similarities to photoionization where the electron perfectly balances the recoil-ion momentum to the extent of the negligibly small momentum transferred by the absorbed photon. In fact, the field of a swift charged projectile can be described as an intense electromagnetic pulse containing a broadband of photon frequencies. In the framework of the Weizsäcker-Williams method target ionization is de-

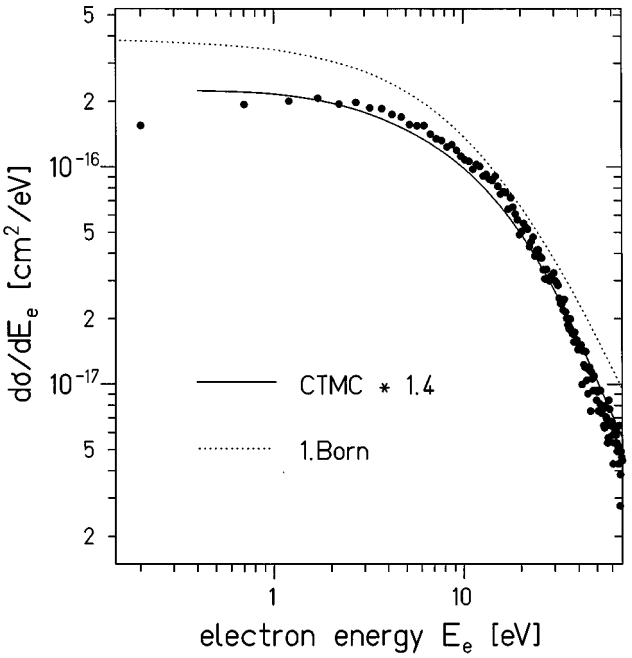

FIG. 4. Singly differential electron emission cross section for single ionization of helium by 3.6 MeV/u Se^{28+}. Full line: CTMC result scaled up by a factor of 1.4. Dotted line: 1.Born approximation [52].

scribed as absorption of those virtual photons by the atom [50]. Since almost no momentum is carried by the incident photons only those whose energy corresponds to the momentum of the electron in the bound state at the instant of absorption can interact. Hence, the obtained momenta of the electrons and the recoil ions are directly related to the internal momenta of the electrons in the helium atom at the instant of the collision with the projectile ion.

The remarkable forward-backward asymmetry of the ionic target fragments can be ascribed to the strong, long-range potential of the outgoing projectile leading to a ''pulling behind'' of the electron and a ''pushing away'' of the remaining target ion (the so-called ''postcollision interaction'': PCI). This behavior is predicted by theory (see Fig. 3). In a recent theoretical study Wood and Olson [51] have shown that the longitudinal emission characteristics of recoil ion and electron change dramatically if the sign of the projectile charge is changed. For antiproton collisions with helium the electron is predicted to be emitted in the backward direction whereas the recoil ion emerges with positive momenta due to the reversed sign of the PCI.

B. Low-energy electrons

The total electron emission is dominated by low-energy electrons with energies well below 50 eV contributing to more than 85% to the total single-ionization cross section. The cross section singly differential in electron energies (integrated over all emission angles) is shown in Fig. 4 in comparison with the theoretical results (full lines) for single ionization of helium by 3.6 MeV/u Se^{28+}. Electrons are coincident with He^{1+} ions and projectiles without charge exchange in their ground state. As in a previous experiment [8] a weak maximum appears around 2 eV which is neither re-

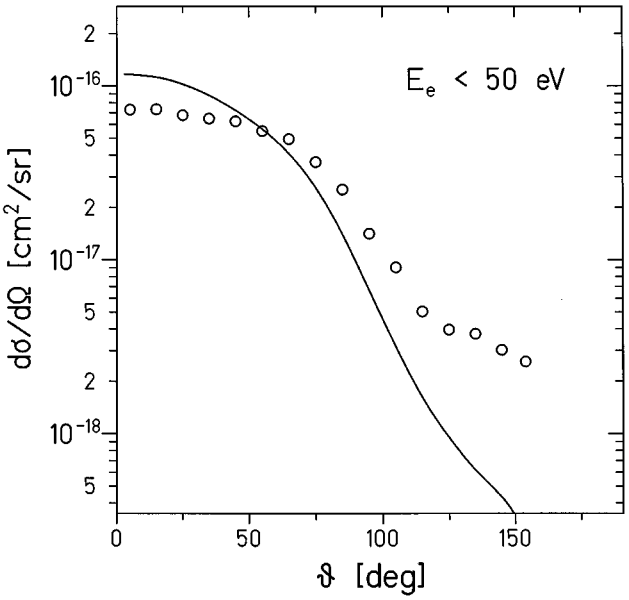

FIG. 5. Singly differential cross section for emission of low-energy electrons with $E_e < 50$ eV as a function of the ejected electron's polar angle. Full line: CTMC calculation multiplied by 1.4.

produced by any theory (Born approximation [52], CTMC) nor by any other experimental investigation. For electron energies above 4 eV the obtained shape of the distribution is in agreement with CTMC, slightly steeper than predicted by the

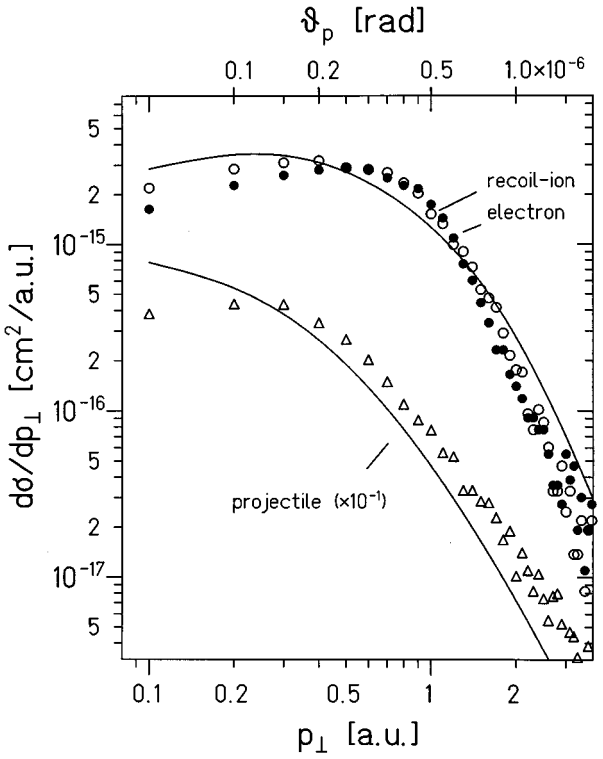

FIG. 6. Transverse momentum distributions of recoil ions, electrons, and projectiles for single ionization of helium. The transverse projectile momentum exchange is directly associated with the scattering angle (upper scale). Smooth lines: CTMC calculation multiplied by 1.4.

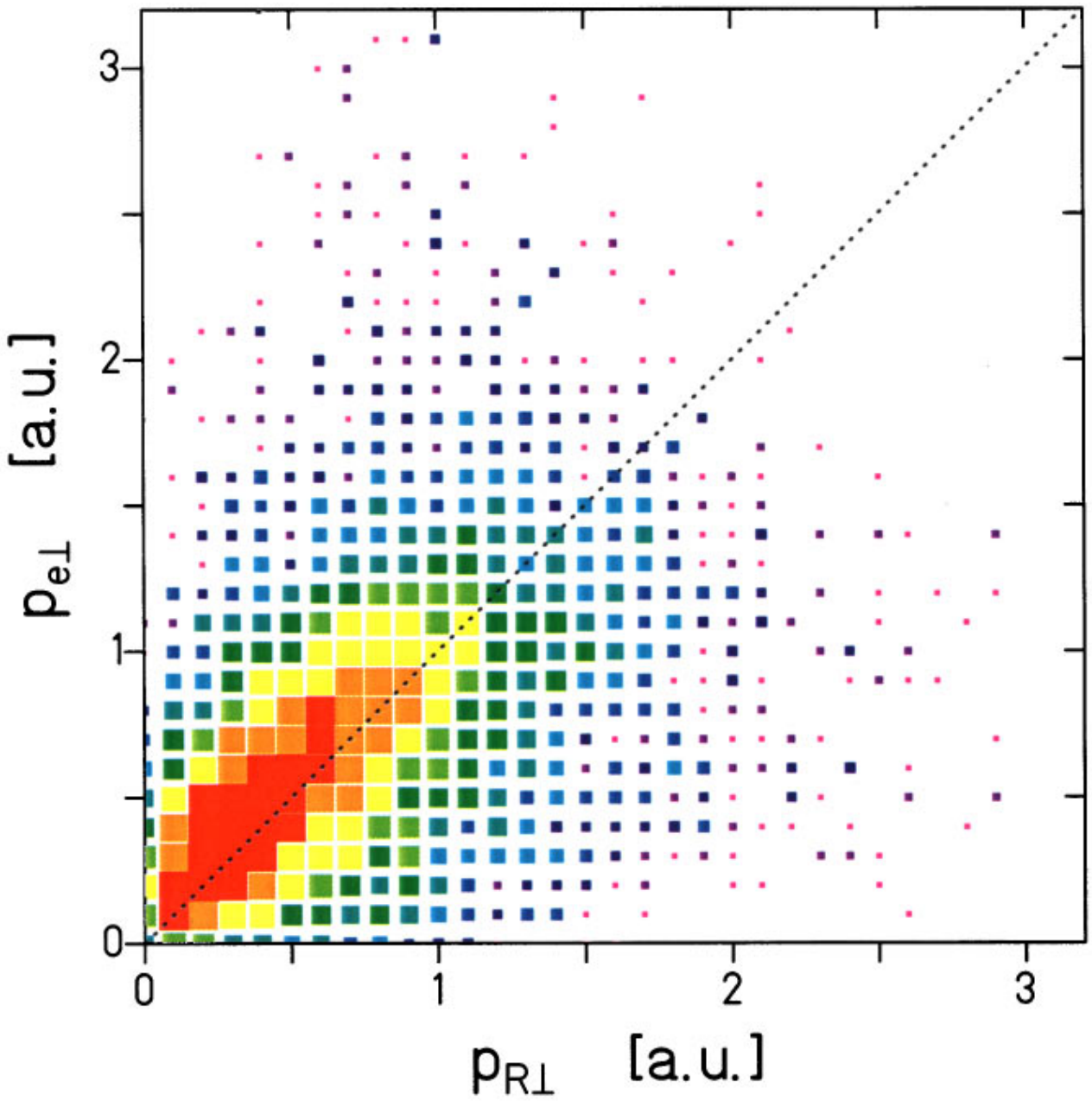

FIG. 7. (Color) $p_{e\perp}$ vs $p_{R\perp}$ for helium single ionization by 3.6 MeV/u Se^{28+} impact. The cluster size represents the doubly differential cross section $d^2\sigma/(dp_{e\perp}dp_{R\perp})$ plotted on a logarithmic scale.

first Born approximation and similar to results of other experimental investigations [53].

We want to emphasize that our results cannot be compared directly to results of any other measurements at low electron energies where neither the final charge state of the projectile nor that of the target was controlled. To the best of our knowledge, the intensity of these very low-energy electrons (the first data point in Fig. 4 comprises all electrons with $0 \leqslant E_e < 400$ meV) has never been investigated experimentally and it is questionable whether some of the electrons in the very low-lying continuum at the target might recombine radiatively. This is one of the questions that will be addressed in further experiments. Reducing the magnitude of the electric extraction and the magnetic guiding fields an energy resolution of a few meV can be achieved with our spectrometer at a bandwidth of $0 \leqslant E_e < 5$ eV. (Such experiments have been performed recently and will be published separately.)

The preference of the forward direction of low-energy electron emission is obvious in the differential cross section as a function of the electron's polar angle (Fig. 5). Here the doubly differential cross section is integrated over electron energies with $E_e < 50$ eV. The angular dependence clearly demonstrates the forward peaked electron emission and a reduction of the cross section by more than one order of magnitude into the backward hemisphere. Although the agreement between experiment and CTMC predictions is quite good for the longitudinal momenta and the electron energies, a slight overestimation is observed in the forward

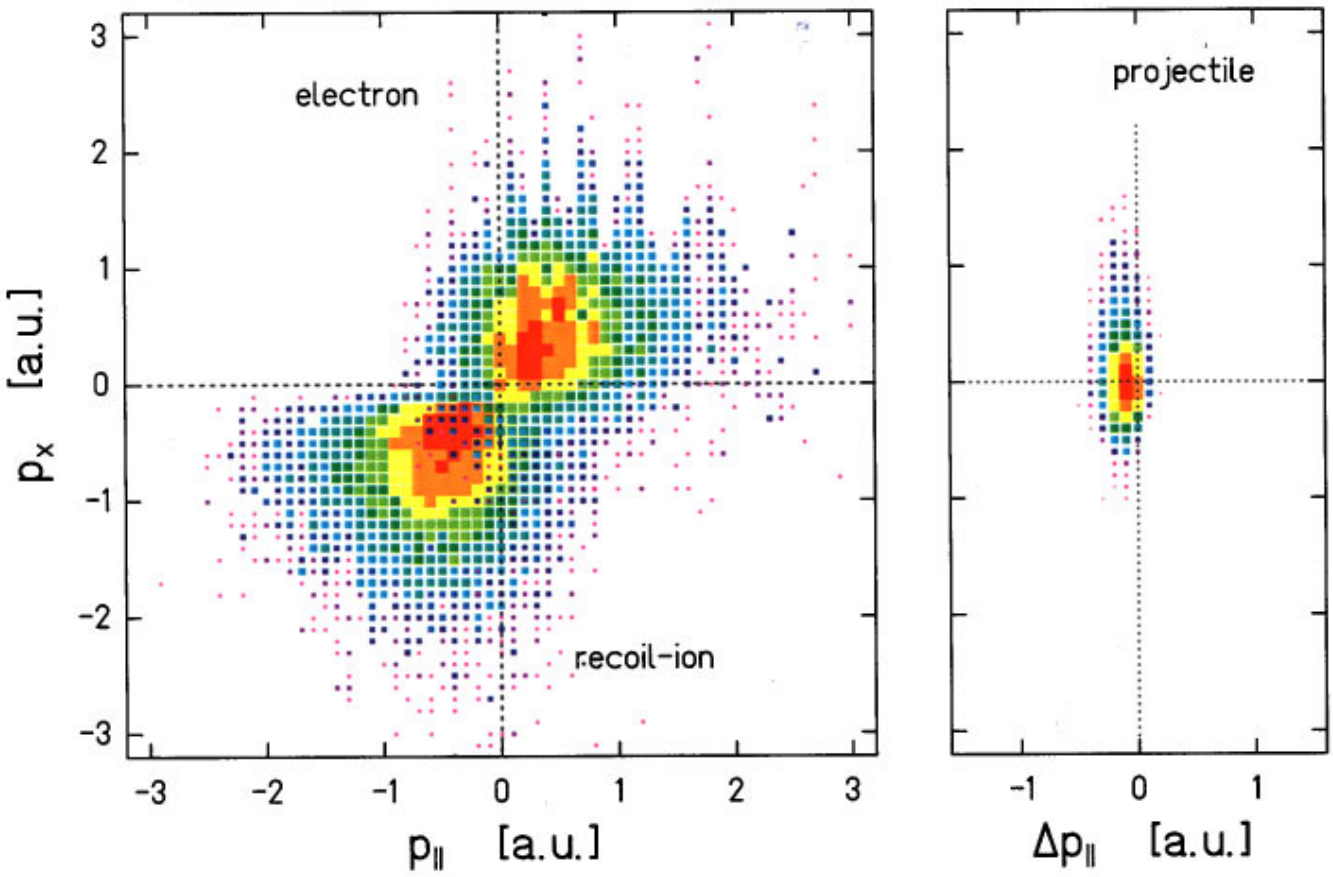

FIG. 8. (Color) Projections in momentum space of all particles in the final state after helium single ionization onto the plane determined by the incident projectile and the outgoing He^{1+} recoil-ion momentum vector (i.e., the collision plane). The cluster size represents the corresponding doubly differential cross section $d^2\sigma/(dp_x dp_\parallel)$ on a logarithmic scale. For the recoil ion this is equal to $d^2\sigma/(dp_{R\perp} dp_{R\parallel})$ since the recoil-ion momentum component pointing out of the paper plane is zero due to the specific projection.

direction along with a significant underestimation of backward emission.

C. Transverse momentum balance

In contrast to the longitudinal direction where recoil-ion and electron momenta are linked via the energy-conservation equation [Eq. (3)] the transverse direction reveals the full three-body dynamics. Here, the transverse recoil-ion momentum compensates the transverse momentum of the ejected electron and in addition the internuclear momentum exchange between the target and the projectile. In Fig. 6 the single-ionization cross section differential in transverse momenta of all outgoing particles is displayed in comparison with predictions obtained from CTMC calculations. We point out that the projectile momentum is deduced from the measured electron and recoil-ion momenta and that the extracted projectile scattering angles in the sub-μrad regime are not accessible by analyzing the outgoing projectile directly. This would require the measurement of a deflection of 1 mm on a detector placed 10 km behind the target region. It would further necessitate a beam quality which is beyond the means of the best available ion accelerators or storage rings.

Surprisingly, within our experimental resolution, there is no difference between the transverse momentum distributions of recoil ions and electrons. Moreover, the transverse momentum transfer to the projectile is smaller than the observed momenta of the atomic fragments. Thus, similarly as in the longitudinal direction they almost completely balance each other. This is possible only if recoil ion and electron are emitted into opposite directions. The experimental results validate the statement that the total momentum transferred by the projectile is small compared to the final momenta of both the ejected electron and recoil ion. One important consequence is that there is no direct relationship between the impact parameter and the transverse recoil-ion momentum or the projectile scattering angle. Theory predicts typical impact parameters for single ionization of about 4 a.u. being larger than the mean spatial extension of the helium atom. Thus, the target nucleus is almost perfectly shielded by its electrons and polarization of the atom becomes important during the inward part of the projectile trajectory which, based on the semiclassical results, should even result in negative deflection angles [30,54]: the projectile was predicted to be scattered to the same side as the emitted recoil ion for a major part of the total single-ionization cross section.

In Fig. 7, where the transverse momentum of the electron is plotted versus that of the recoil ion, those events would appear above the diagonal line with $p_{R\perp} = p_{e\perp}$. This is true only if electron and recoil ion are perfectly emitted back to back in the azimuthal plane (the plane perpendicular to the projectile beam), which will be discussed in more detail in one of the following sections. In conclusion, the momenta of

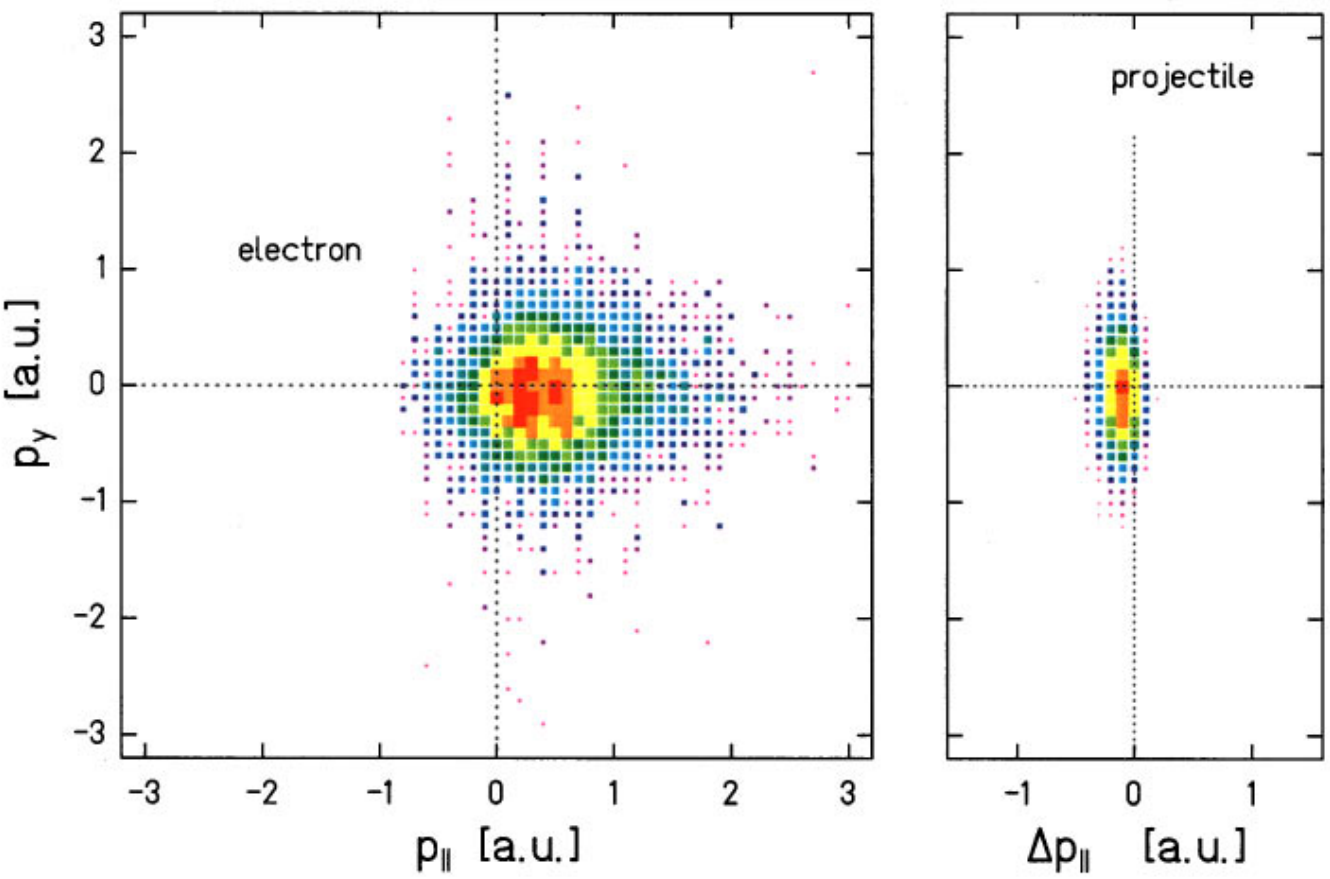

FIG. 9. (Color) Momenta of emitted electron and scattered projectile projected onto the $(p_y\text{-}p_\parallel)$ plane. In this representation the outgoing recoil-ion momentum vector stands perpendicular to the paper plane corresponding to a rotation of the coordinate system defined in Fig. 8 by 90° around the $p_\parallel$ axis (i.e., a ''side view'' of Fig. 8). Plotted are the doubly differential cross sections $d^2\sigma/(dp_y dp_\parallel)$ for the electron and projectile ions, respectively, on a logarithmic scale.

electron and recoil ion are strongly coupled in the longitudinal as well as in the transverse direction: if the electron is emitted with a high momentum then the recoil-ion momentum is also large. In addition, for the overwhelming part of all collision events the momentum transfer from the projec tile is comparably small. This is true in the transverse as well as in the longitudinal direction.

D. Three-particle dynamics

A convenient representation to illuminate the complete three-particle momentum balance is to project the momenta of all outgoing reactants onto the collision plane (see Fig. 2) defined by the incident projectile ($p_\parallel$ direction) and the transverse recoil-ion momentum vector ($-p_x$ direction) (Fig. 8). Several of the main features characterizing the dynamics of target single ionization by fast heavy ions can be deduced from this representation. First, the forward-backward asymmetry of recoil ion and electron which, according to theory, is a result of the long-range interaction with the receding projectile ion (PCI effect). Second, the momentum imparted by the projectile is small in comparison to the momenta of the atomic fragments revealing similarities with ionization by photoabsorption. Third, the recoil ion and electron are preferably emitted back to back balancing their momenta on a level which corresponds to the small momentum transferred by the projectile.

The tail observed in the projectile distribution towards positive p_x momenta in Fig. 8 can be attributed to the direct interaction of the projectile with the target nucleus. Only for those encounters is the momentum transfer related to the impact parameter, but this is a minor fraction of all collisions leading to single ionization of helium (cross sections are on a logarithmic scale in Fig. 8). This fact is further supported by the representation chosen in Fig. 9 where the recoil-ion momentum vector is pointing out of the paper plane. Here electron and projectile momenta are projected perpendicularly to the above defined collision plane corresponding to a ''side view'' of Fig. 8 from the x direction. If the projectile deflection would be caused mainly by interaction with the target nucleus this projection would deliver narrow distributions centered along the p_z axis. Instead, a considerable amount of momentum transfer out of the collision plane is observed experimentally. This implies that the recoil ion and electron are not perfectly emitted back to back. Moreover, the azimuthal angle enclosed by the electron and recoil ion should show a distinct distribution. This point together with the angular correlation between all participating particles in the azimuthal plane will be discussed in more detail in the following section.

There has been a lively recent discussion on the so-called ''asymmetry of the soft electron emission'' in collisions with strong perturbations. Analyzing data sampled with conven-

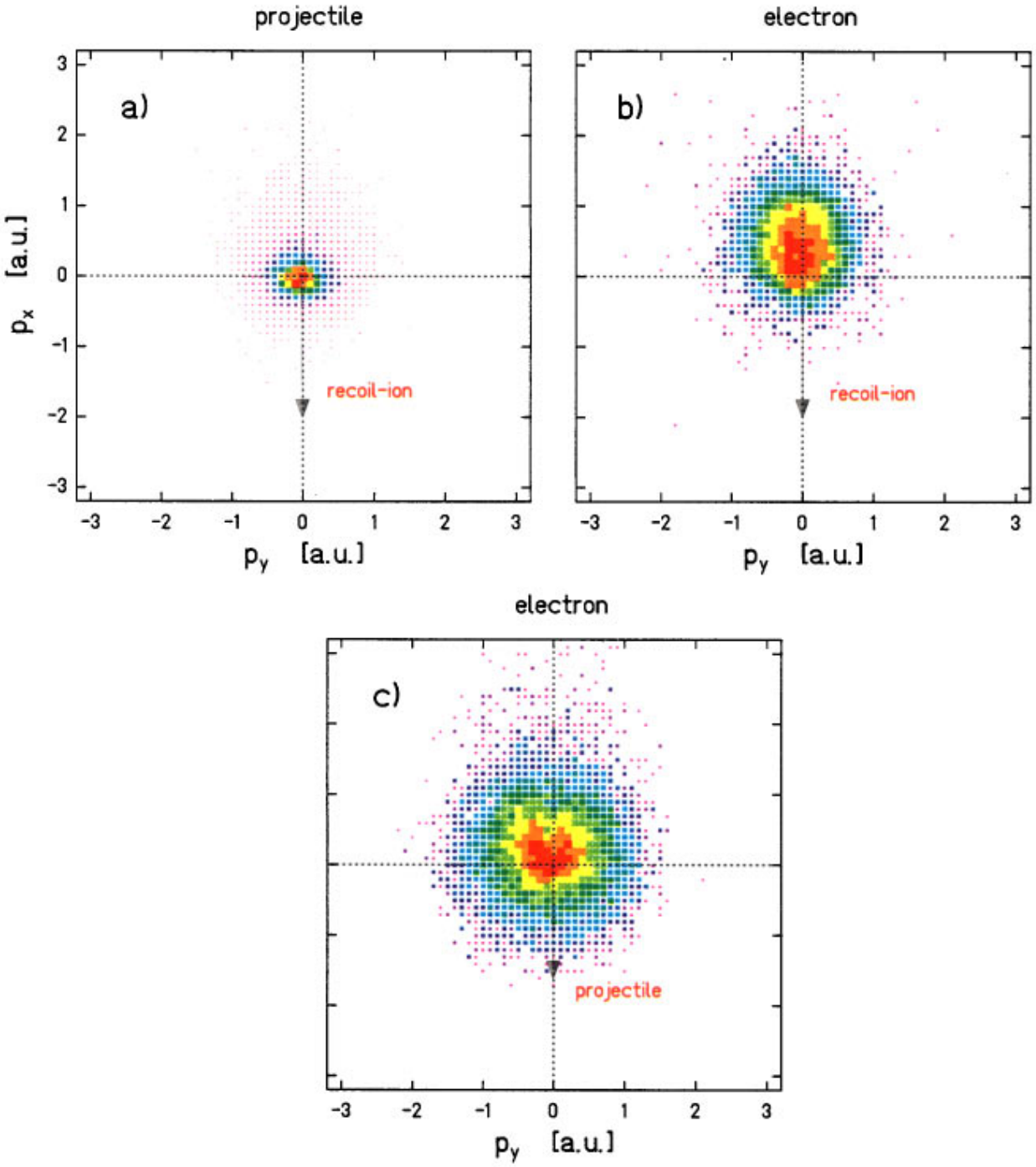

FIG. 10. (Color) The momenta of (a) outgoing projectile ion and (b) ejected electron projected onto the azimuthal plane (the plane perpendicular to the incoming projectile velocity vector). The orientation is defined by the He^{1+} recoil ion which is scattered along the negative p_x axis as indicated by the arrows. In (c) the projected electron momentum distribution is shown with respect to the scattered projectile which is deflected towards the negative p_x direction defining the rotation in this plot. The doubly differential cross sections $d^2\sigma/(dp_x dp_y)$ are presented on a logarithmic scale.

tional electron spectrometers for electron energies above 1 eV [2], it was found that most of these electrons are emitted into the forward direction as a result of two-center effects [53,55]. Exploring the full three-particle collision dynamics with our method illuminates that this asymmetry indeed is twofold. In addition to the distinct forward emission of the soft electrons another asymmetry becomes obvious in that the maximum of the electron momentum distribution in the scattering plane is found opposite to the recoil-ion emission. As will be shown in a subsequent theoretical paper this characteristic changes dramatically as a function of the collision velocity.

E. Azimuthal angular correlations

In this section we want to restrict the discussion to projections of the full three-particle momentum space obtained

after helium single ionization onto the azimuthal plane, the plane perpendicular to the incoming projectile velocity vector [i.e., the $(p_x\text{-}p_y)$ plane according to the convention used so far]. The projections of the outgoing projectile and the emitted electron momentum with respect to the recoil ion are displayed in Figs. 10(a) and 10(b). The distributions are oriented such that the momentum vector of the scattered He^{1+} recoil ion is pointing along the negative p_x direction as indicated by the arrows without additional condition on the length of this vector.

A very narrow distribution centered around the origin is obtained for the projectile ion demonstrating again the weak momentum exchange between projectile and target nucleus. Helium single ionization is dominated by small-angle scattering of the projectile which is deflected almost isotropically with respect to the recoiling target nucleus. Moreover, with finite probability negative scattering angles occur and the projectile is scattered to the recoil-ion side ($-p_x$ direction). Within the experimental resolution for the projectile momentum change of about $\Delta p_{p\perp} \approx \pm 0.1$ a.u. corresponding to a polar scattering angle resolution of $\Delta \vartheta_p \approx \pm 57$ nrad no significant shift of the center of the projectile scattering distribution towards the recoil-ion side can be observed.

A quite different behavior is obtained for the ejected electron to be emitted preferentially into the opposite direction of the recoil ion [Fig. 10(b)]. Thus, we again observe a strong linkage between recoil ion and electron but, on the other hand, there is almost no azimuthal angular correlation between the projectile and the ionic target fragments. This is illuminated by plotting the electron momentum distribution projected onto the azimuthal plane with respect to the scattered projectile in Fig. 10(c). Only a weak correlation is observed such that the electrons slightly tend to be scattered opposite to the projectile. For a better comparison these results are compiled in the polar diagrams of Fig. 11 showing the corresponding angular distributions for the azimuthal angles between all ejected reactants.

Exploring the characteristics of the three-particle momentum exchange in even more detail, it is instructive to plot the azimuthal angle between recoil ion and electron φ_{re} versus the angle enclosed by recoil ion and projectile φ_{rp} calculated for each single event (Fig. 12). In this representation the different collision mechanisms contributing to target single ionization can be separated in a simple and illustrative manner since the dominance of any possible two-body interaction can be assigned to specific regions in this plot. For the occurrence of a direct nucleus-nucleus interaction, where the electron takes up the part of a spectator, recoil ion and projectile are emitted back to back into opposite directions. Thus those events are characterized to appear along the line with $\varphi_{rp} = 180°$. Following the same argumentation binary encounter electron emission, which is a two-body interaction between projectile and electron, shows up along the diagonal $\varphi_{rp} = 180° - \varphi_{re}$, whereas a strong coupling of recoil ion and electron, which can be associated with ''photoionization,'' appears with the typical angle of $\varphi_{re} = 180°$. All events inside these boundary lines experience momentum exchange between all participating particles on the basis of a three-body interaction. Thus, the observed pattern clearly demonstrates the importance of the three-body momentum exchange. It also shows, however, that the kinematics of single ionization by fast heavy-ion impact is dominated by electronic dipole transitions where the recoil-ion electron two-body interaction dominates the three-body momentum exchange.

Many of the discussed features, such as the small momentum loss of the projectile, the preferred back to back emission of the recoil ion and electron, and the fact that the observed momenta compare well to the internal momenta of the target atom, are inherently included in the simple picture where ionization is the result of the interaction with the equivalent photon field of the passing projectile ion. Although the Weizsäcker-Williams formalism and the first-order Born approximation fail in reproducing, e.g., the total cross section for the present collision system since they are valid only in the limit of high velocities (at large v_p and small perturbations both formulations are identical), the assumption that dipole excitations contribute mainly to ionization is still valid in the present regime of fast collisions with large perturbation strengths.

V. CONCLUSIONS

We have performed a kinematically complete experiment for single ionization of helium by charged particle impact using advanced many particle detection techniques. The full momentum vectors of all participating reactants were measured with high resolution and the dynamics of helium single ionization by fast heavy ions was explored. The results of our work are manyfold.

First, a fast highly charged projectile is an extremely ''soft'' and ''sensitive'' tool to ionize the target. It merely transfers momentum to the target electrons, acting very much like a photon field. Moreover, since no momentum or energy exchange between the two electrons is required to obtain double ionization the final two electron momentum distribu-

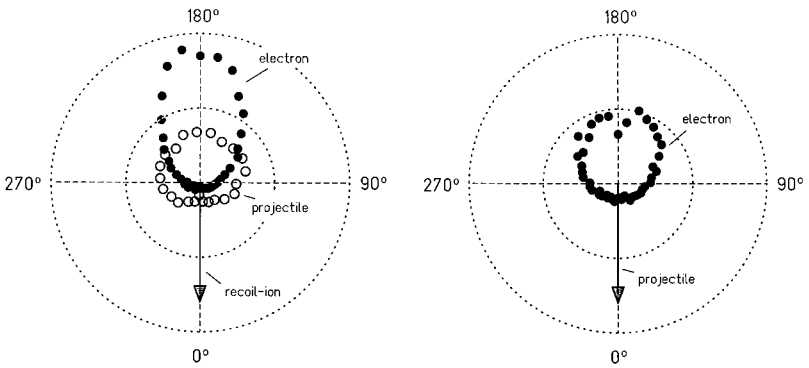

FIG. 11. The angular distributions between the three outgoing particles in the azimuthal plane perpendicular to the initial projectile direction. Polar representation of the singly differential cross section as function of the azimuthal angle $d\sigma/d\varphi$ between the transverse momentum vectors of the specified particles.

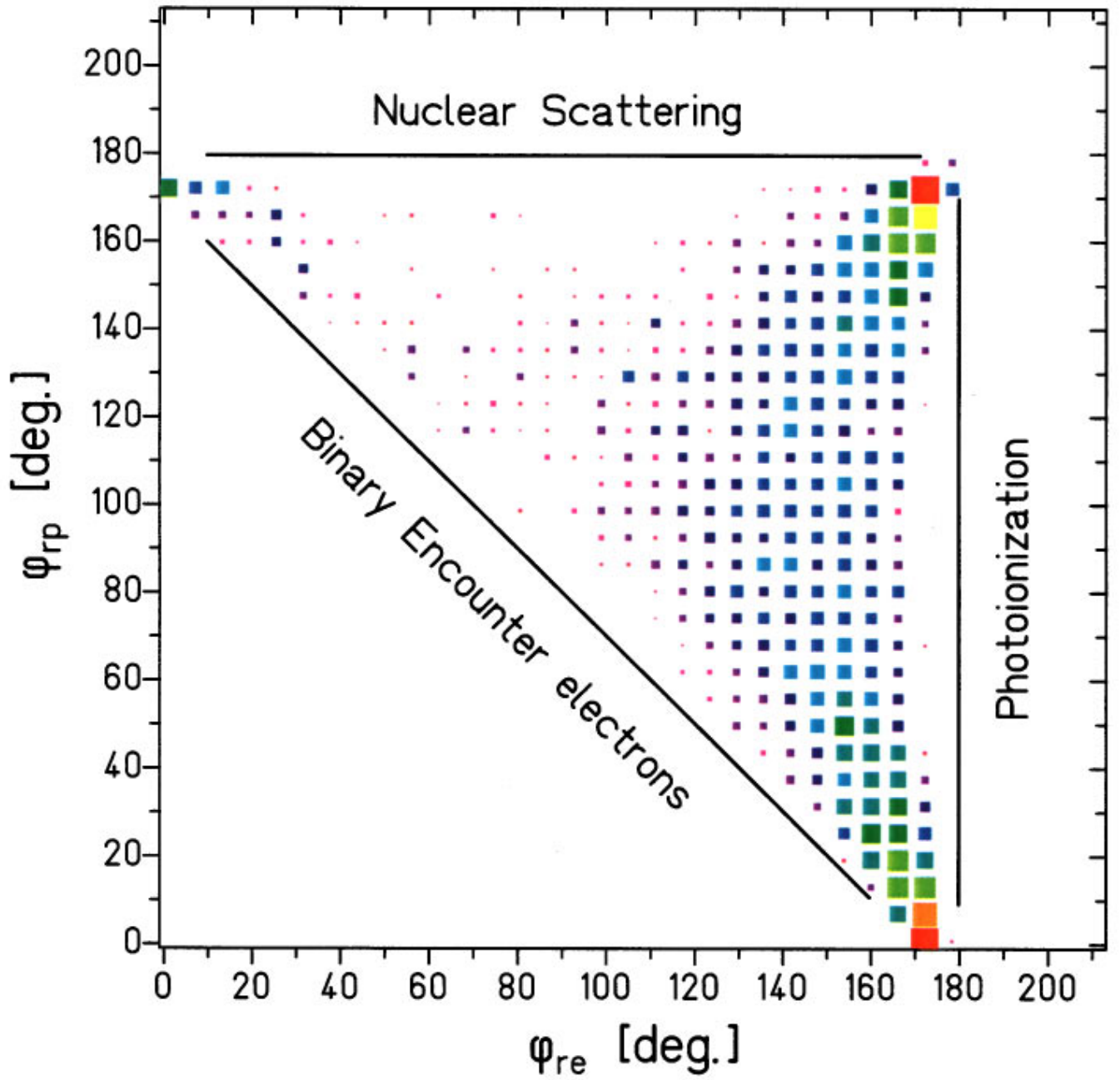

FIG. 12. (Color) The azimuthal angle between recoil ion and electron plotted vs that between recoil ion and projectile. Indicated are the kinematical lines assuming the specified two-body interactions and considering the third particle as a spectator (see text). The region below the diagonal line is forbidden because of simple kinematical reasons.

tions have been demonstrated to be a sensitive probe of the (e-e) correlation in the ground state as well as during the collision [44].

Second, the strong and long-ranging potential of the outgoing projectile ion causes a considerable forward-backward asymmetry of the recoil ion and electron. The asymmetry of the electron emission which has been discussed before is found to be twofold: In addition to being scattered forward the electrons are emitted opposite to the recoil ion in the scattering plane. One can easily show that, for the present situation, all particles strongly interact in the continuum, which is an ideal situation to investigate the three-body Coulomb continuum. As expected, semiclassical calculations inherently including all the interactions among the particles, correctly describe the continuum.

Third, the attempt to separate the many particle problem into several two-body interactions shows that for the present collision system the strongest correlation occurs between the recoil ion and the electron and not, as might be expected, between the recoil ion and the projectile via nuclear Coulomb deflection. Thus, and very importantly, it is definitely impossible for the major part of all collisions resulting in single ionization to extract the impact parameter from the observable quantities. This has been demonstrated before for proton on helium singly ionizing collisions at energies between 0.5 MeV [18] and 3.0 MeV [16,56], i.e., at consider-

ably smaller perturbations. As far as theories are concerned, many particle interactions between the electrons and the nuclei have to be incorporated and the impact-parameter formulation using a classical trajectory in the (screened) potential of the target is not adequate for the present situation. Recent experiments and calculations [27] show that such an approximation may be partly applicable for single ionization at very low projectile velocities comparable to orbital velocity of outer-shell electrons.

Fourth, the comparisons with results obtained from CTMC calculations demonstrate that this semiclassical model is reliably applicable in the present regime of high perturbations. In spite of the approximative description of bound many electron atomic states (actually this is also true for all quantal calculations on bound many electron states) it clearly predicts the underlying collision dynamics and allows the extraction of highly differential cross sections. It is the only model available that includes many particle interactions and the coupling between electronic and nuclear motion in a consistent way. The inclusion of the full $(e\text{-}e)$ interaction during the collision and in the final state was shown to be essential to come to a reasonable agreement with experimental data in the case of double ionization [44].

VI. FUTURE PERSPECTIVES

Since several other experimental groups are now using similar techniques, in the near future many new experiments will be performed over the wide range of projectile energies available at different accelerator facilities. As will be detailed in a subsequent theoretical paper the characteristics of the three-body collision dynamics undergo dramatic changes as a function of v_p and q_p. Regimes are found where any of the mutual two-body interactions dominate the three-particle momentum exchange as well as ''true'' three-body situations are present. A flavor of the rich variety to be expected can be obtained by comparing the present results with a similar experiment for 5–15 keV proton impact on helium [57]. Therefore, it would be most desirable that full three-particle quantum-mechanical calculations are developed in the near future giving consistent results over the whole range of perturbations.

Even more, applying our experimental technique, it is to be expected that the complete momentum vectors of up to five continuum electrons emerging from a collision can be determined simultaneously in the near future. The first kinematically complete experiment on helium double ionization has been already performed [44] and further results will be published soon. They certainly will be followed by more investigations using protons or electrons as projectiles, as is summarized in an upcoming review on the field of recoil-ion momentum spectroscopy [23].

Recently similar experiments have been performed using 1 GeV/u U^{92+} projectiles from the SIS (heavy-ion synchrotron) at GSI extending the investigations to the highest possible perturbation in the high velocity limit. (The results will be published separately in a forthcoming paper.) Then, on one hand, relativistic effects become important and especially the magnetic interaction of the relativistic projectile with the target might be strong enough to considerably modify the collision dynamics. At the same time, the modification of the electron spectra by the final-state interaction with the receding projectile will be reduced by at least a factor of 5, so that the mapping of the correlated motion of the electrons from the initial to the final state is expected to be less influenced by PCI.

We would like to emphasize that fast GeV/u highly charged ions are a unique, unsurpassed source of light delivering attosecond (10^{-18} sec), exawatt/cm^2 (10^{18} W/cm^2), and broadband pulses of virtual photons. These features have been exploited in nuclear physics to investigate nuclear structure (halo nuclei, giant resonances, etc.). Combined with kinematically complete experiments on double (multiple) ionization this reveals an ''attosecond microscope'' for the investigation of the correlated many-electron motion within parts of typical revolution times in bound states. In addition, molecules, clusters, or even solids can be used as targets. Thus, one might envisage that this method will become a standard technique for the investigation of bound-state many-electron correlations in atoms, molecules, clusters, and solids.

ACKNOWLEDGMENTS

This work was supported by GSI, DFG, and BMFT. We would like to thank our colleagues and friends A. Cassimi, C. L. Cocke, R. Dörner, S. Hagmann, M. Horbatsch, O. Jagutzki, S. Keller, R. Mann, V. Mergel, and L. Spielberger for many stimulating discussions. The excellent work of the UNILAC crew of GSI for providing the ion beam and the technical support by A. Bardonner are acknowledged. The authors would like to thank the Alexander von Humboldt Stiftung for their support and acknowledge the financial support of NATO.

[1] M. E. Rudd, Y. Kim, D. H. Madison, and T. J. Gay, Rev. Mod. Phys. **64**, 441 (1992).

[2] H. Platten, G. Schiwietz, T. Schneider, D. Schneider, W. Zeitz, K. Musiol, T. J. M. Zouros, R. Kowallik, and N. Stolterfoht, in *Fifteenth International Conference on the Physics of Electronic and Atomic Collisions, Abstracts*, edited by J. Geddes *et al.* (University Press, Brighton, 1987).

[3] L. C. Tribedi, P. Richard, Y. D. Wang, C. D. Lin, and R. E. Olson, Phys. Rev. Lett. **77**, 3767 (1996).

[4] I. E. McCarthy and E. Weigold, Rep. Prog. Phys. **54**, 789 (1991).

[5] S. Suárez, C. Garibotti, W. Meckbach, and G. Bernardi, Phys. Rev. Lett. **70**, 418 (1993).

[6] N. Stolterfoht, R. D. DuBois, and R. D. Rivarola, Rev. Mod. Phys. (to be published).

[7] G. Kraft, Nucl. Sci. Appl. **3**, 1 (1987).

[8] R. Moshammer, J. Ullrich, M. Unverzagt, W. Schmitt, P. Jardin, R. E. Olson, R. Mann, R. Dörner, V. Mergel, U. Buck, and H. Schmidt-Böcking, Phys. Rev. Lett. **73**, 3371 (1994).

[9] O. Schwarzkopf, B. Krässig, J. Elminger, and V. Schmidt, Phys. Rev. Lett. **70**, 3008 (1993).

[10] W. T. Htwe, T. Vajnai, M. Bernhart, A. D. Gaus, and M.

Schulz, Phys. Rev. Lett. **73**, 1348 (1995).
[11] H. Schöne, R. Schuch, S. Datz, M. Schulz, P. F. Dittner, J. P. Giese, Q. C. Kessel, H. F. Krause, P. D. Miller, and C. R. Vane, Phys. Rev. A **51**, 324 (1995).
[12] R. Schuch, H. Schöne, P. D. Miller, H. F. Krause, P. F. Dittner, S. Datz, and R. E. Olson, Phys. Rev. Lett. **60**, 925 (1988).
[13] G. Schiwietz, B. Skogvall, J. Tanis, and D. Schneider, Phys. Rev. A **38**, 5552 (1988).
[14] S. Kelbch, C. L. Cocke, S. Hagmann, M. Horbatsch, C. Kelbch, R. Koch, H. Schmidt-Böcking, and J. Ullrich, J. Phys. B **22**, 1277 (1989).
[15] V. Frohne, S. Cheng, R. Ali, M. Raphaeilian, C. L. Cocke, and R. E. Olson, Phys. Rev. Lett. **71**, 696 (1993).
[16] A. Gensmantel, J. Ullrich, R. Dörner, R. E. Olson, K. Ullmann, E. Forberich, S. Lencinas, and H. Schmidt-Böcking, Phys. Rev. A **45**, 4572 (1992).
[17] R. Dörner, J. Ullrich, H. Schmidt-Böcking, and R. E. Olson, Phys. Rev. Lett. **63**, 147 (1989).
[18] S. Lencinas, J. Ullrich, R. Dörner, R. E. Olson, W. Wolff, L. Spielberger, S. Hagmann, M. Horbatsch, C. L. Cocke, and H. Schmidt-Böcking, J. Phys. B **26**, 287 (1993).
[19] P. Jardin, A. Cassimi, J. P. Grandin, H. Rothard, J. P. Lemoigne, D. Hennecart, X. Husson, and A. Lepoutre, Nucl. Instrum. Methods Phys. Res. B **98**, 363 (1995).
[20] J. Ullrich, R. Dörner, V. Mergel, O. Jagutzki, L. Spielberger, and H. Schmidt-Böcking, Comments At. Mol. Phys. **30**, 285 (1994).
[21] V. Mergel, R. Dörner, J. Ullrich, O. Jagutzki, S. Lencinas, S. Nüttgens, L. Spielberger, M. Unverzagt, C. L. Cocke, R. E. Olson, M. Schulz, U. Buck, E. Zanger, W. Theisinger, M. Isser, S. Geis, and H. Schmidt-Böcking, Phys. Rev. Lett. **74**, 2200 (1995).
[22] A. Cassimi, S. Duponchel, X. Flechard, P. Jardin, P. Sportais, D. Hennecart, and R. E. Olson, Phys. Rev. Lett. **76**, 3679 (1996).
[23] J. Ullrich, R. Moshammer, R. Dörner, O. Jagutzki, V. Mergel, H. Schmidt-Böcking, and L. Spielberger, J. Phys. B (to be published).
[24] R. Moshammer, M. Unverzagt, W. Schmitt, J. Ullrich, and H. Schmidt-Böcking, Nucl. Instrum. Methods Phys. Res. B **108**, 425 (1996).
[25] M. Pieksma, S. Y. Ovchinnikov, J. van Eck, W. B. Westerwald, and A. Niehaus, Phys. Rev. Lett. **73**, 46 (1994).
[26] S. D. Kravis, M. A. Abdallah, C. L. Cocke, C. D. Lin, M. Stöckli, B. Walch, Y. D. Wang, R. E. Olson, V. D. Rodriguez, W. Wu, M. Pieksma, and N. Watanabe, Phys. Rev. A **54**, 1394 (1996).
[27] R. Dörner, H. Khemliche, M. H. Prior, C. L. Cocke, J. A. Gary, R. E. Olson, V. Mergel, J. Ullrich, and H. Schmidt-Böcking, Phys. Rev. Lett. **77**, 4520 (1996).
[28] P. D. Fainstein, V. H. Ponce, and R. D. Rivarola, J. Phys. B **24**, 3091 (1991).
[29] M. Horbatsch and R. M. Dreizler, Phys. Lett. **113A**, 251 (1985).
[30] R. E. Olson, J. Ullrich, and H. Schmidt-Böcking, Phys. Rev. A **39**, 5572 (1989).
[31] U. Fukuda, I. Shimamura, L. Vegh, and T. Watanabe, Phys. Rev. A **44**, 1565 (1991).
[32] A. Salin, J. Phys. B **24**, 3211 (1991).
[33] X. Fang and J. F. Reading, Nucl. Instrum. Methods Phys. Res. B **53**, 453 (1991).
[34] S. Y. Ovchinnikov and J. H. Macek, Phys. Rev. Lett. **75**, 2474 (1995).
[35] D. R. Schultz, P. S. Krstić, C. O. Reinhold, and J. C. Wells, Phys. Rev. Lett. **76**, 2882 (1996).
[36] M. Chassid and M. Horbatsch, J. Phys. B (to be published).
[37] N. Stolterfoht, H. Platten, G. Schiwietz, D. Schneider, L. Gulyas, P. D. Fainstein, and A. Salin, Phys. Rev. A **52**, 3796 (1995).
[38] P. Jardin, A. Cassimi, J. P. Grandin, D. Hennecart, and J. P. Lemoigne, Nucl. Instrum. Methods Phys. Res. B **107**, 41 (1996).
[39] M. Unverzagt, R. Moshammer, W. Schmitt, R. E. Olson, P. Jardin, V. Mergel, J. Ullrich, and H. Schmidt-Böcking, Phys. Rev. Lett. **76**, 1043 (1996).
[40] J. H. McGuire, A. Müller, B. Schuch, W. Groh, and E. Salzborn, Phys. Rev. A **35**, 2479 (1987).
[41] A. Salin, Phys. Rev. A **36**, 5471 (1987).
[42] V. D. Rodriguez, Y. D. Wang, and C. D. Lin, J. Phys. B **28**, L471 (1995).
[43] V. J. Montemayor and G. Schiwietz, Phys. Rev. A **40**, 6223 (1989).
[44] R. Moshammer, J. Ullrich, H. Kollmus, W. Schmitt, M. Unverzagt, O. Jagutzki, V. Mergel, H. Schmidt-Böcking, C. J. Wood, and R. E. Olson, Phys. Rev. Lett. **77**, 1242 (1996).
[45] H. Kollmus, W. Schmitt, R. Moshammer, M. Unverzagt, and J. Ullrich, Nucl. Instrum. Methods Phys. Res. B **124**, 377 (1997).
[46] S. Sobottka and M. Williams, IEEE Trans. Nucl. Sci. **35**, 1 (1980).
[47] S. Schippers, R. Hoekstra, R. Morgenstern, and R. E. Olson, J. Phys. B **29**, 2819 (1996).
[48] Y. D. Wang, V. D. Rodriguez, C. D. Lin, C. L. Cocke, S. Kravis, M. Abdallah, and R. Dörner, J. Phys. A **53**, 3278 (1996).
[49] H. Berg *et al.*, J. Phys. B **25**, 3655 (1992).
[50] E. J. Williams, Phys. Rev. **45**, 729 (1934); J. D. Jackson, *Classical Electrodynamics* (Wiley, New York, 1975).
[51] C. J. Wood and R. E. Olson, J. Phys. B **29**, L257 (1996).
[52] D. S. F. Crothers and M. McCartney, Comput. Phys. Commun. **72**, 288 (1992).
[53] J. O. P. Pedersen, P. Hvelplund, A. G. Petersen, and P. D. Fainstein, J. Phys. B **24**, 4001 (1991).
[54] M. Horbatsch, Phys. Lett. A **137**, 466 (1989).
[55] F. D. Covalecchia, W. Cravero, and C. R. Garibotti, Phys. Rev. A **52**, 3737 (1995).
[56] E. Y. Kumber, C. L. Cocke, S. Cheng, and S. L. Varghese, Phys. Rev. Lett. **60**, 2026 (1988).
[57] R. Dörner, V. Mergel, L. Spielberger, M. Achler, Kh. Khayyat, T. Vogt, H. Bräuning, O. Jagutzki, T. Weber, J. Ullrich, R. Moshammer, M. Unverzagt, W. Schmitt, H. Khemliche, M. Prior, C. L. Cocke, J. Feagin, R. E. Olson, and H. Schmidt-Böcking, Nucl. Instrum. Methods Phys. Res. B **124**, 225 (1997).